CW SAR SIGNAL MODEL AND SYSTEM IMPLEMENTATION

Andon Lazarov, Dimitar Minchev
Burgas Free University

***Abstract**: Synthetic Aperture Radar (SAR) problem referred to image reconstruction of a moving target and SAR implementation is considered. Three-dimensional (3-D) SAR geometry is analytically described. The target is presented as an assembly of point scatterers. Mathematical expressions to calculate the range distance from SAR to each point scatterer are derived. SAR signal model based on a linear frequency modulated continuous wave emitted signal, 3-D geometry and reflectivity function of the target is derived. Image reconstruction procedure based on Fourier transform for range compression and azimuth compression is applied. Polynomial autofocusing algorithm for SAR imaging of a moving target is suggested. Mini SAR system is implemented and experimental results are provided.*

***Keywords:** SAR geometry, SAR Digital Signal Processing, SAR Signal Model, SAR Implementation.*

МОДЕЛ НА СИГНАЛ С НЕПРЕКЪСНАТА ЛИНЕЙНО ЧЕСТОТНА МОДУЛАЦИЯ И ИМПЛЕМЕНТАЦИЯ НА РАДИОЛОКАЦИОННА СИСТЕМА СЪС СИНТЕЗИРАНА АПЕРТУРА

Андон Лазаров, Димитър Минчев
Бургаски свободен университет

***Резюме:** Представен е модел на сигнал с непрекъсната линейно честотна модулация и имплементация на радиолокационна система със синтезирана апертура. Дефинирани са геометрията и основните кинематични уравнения, описващи топологията на SAR. Изведена е процедурата за възстановяване на образа. Имплементирана е SAR система.*

***Ключови думи:** Геометрия на SAR, цифрова обработка на SAR сигнали, SAR модел на радар, имплементация на SAR радар.*

1. Introduction

SAR systems provide mapping of Earth and ocean surface and imaging of stationary and moving targets on them as well. Wide bandwidth signals are used to realize range resolution while the motions of the radar platform and target induce an azimuth resolution, but the accuracy of the processing is dependent on proper autofocusing procedure. Image extraction range Doppler technique requires determination of portion of signal to be compressed. It can be easily achieved by applying a pulse mode of the radar transmitter. A drawback arises while continuous emitted waveform is applied in order to realize a range resolution. SAR systems are designed and built for a decade and a number of works in the field of SAR design have emerged [1,2], describing the theory of pulse modulation and transmitted waveforms, detection theory including matched filter detection, basic antenna

theory, and signal-to-noise ratio calculations. In [1] a discussion of end-to-end system design is provided including signal generation, antenna considerations, sampling and data storage, and data processing techniques. Small pulsed SAR systems [3] low-power CW systems [4] have been designed. More recent literature on SAR exists as well. The theory of SAR and outlines important design considerations for space borne systems is explained in [5]. The design of new SAR systems has been outlined in [6, 7, 8]. SAR signal processing has been discussed in [9, 10]. The development includes the use of active and passive targets on a predetermined calibration site to measure transmitted power, antenna beam pattern, and signal-to-noise ratio. The author of work [11] on the measurement of radar cross section provides information concerning ground-based range measurements. It includes particularly insightful sections on accounting for effects caused by the antenna beam pattern and ground plane. Design and development of a C-band RF transceiver for UAVSAR is described in [12].

The problem of air borne (space born) side-view SAR imaging of moving target with CW - continuous linear frequency modulation waveform is explored in the present work. The main objectives are to develop the geometry of SAR scenario, to determine the basic geometrical characteristic of SAR scenario, to propose CW linear frequency modulated SAR signal model and image reconstruction, and autofocusing procedure. The goal of the processing is to achieve a side view of the target which is of particular interest for further classification purposes. The focus of the analysis is on the definition of CW triangle linear frequency modulated SAR signal, image reconstruction techniques, and geometry description of SAR scenario with the moving target and SAR implementation. The main result of this work is adequate 3-D geometry of the SAR scenario described by analytical geometrical expressions, CW SAR signal models with linear frequency modulation, robust image reconstruction processing scheme including, range and azimuth compression, polynomial autofocusing phase correction with entropy image quality evaluation, which allow optimal target shape extraction and SAR system implementation.

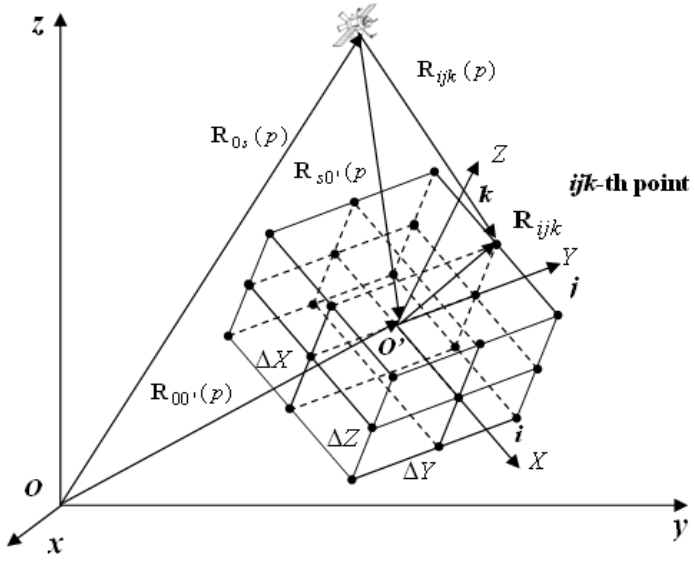

Fig. 1. *The geometry of SAR scenario*

2. Geometry of SAR scenario

Consider general case of airborn (spaceborn) SAR illuminating a moving target. The topology is depicted in a reference coordinate system of observation $Oxyz$, the origin of which, point O, is placed beneath the radar platform. The target is presented as an assembly of point scatterers placed in the nods of a 3-D regular grid in coordinate system $O'XYZ$.

Based on the geometry in Fig. 1 the following equations can be written:
The range distance vector from the SAR to the mass center of the target

$$\mathbf{R}_{s0'}(p) = \mathbf{R}_{0s}(p) - \mathbf{R}_{00'}(p), \tag{1}$$

$$\text{where } \mathbf{R}_{00'}(p) = \mathbf{R}_{00'}(0) - \mathbf{V}_{0'}\left(\frac{N}{2} - p\right)T_p, \tag{2}$$

$$\mathbf{R}_{0s}(p) = \mathbf{R}_{0s}(0) + \mathbf{V}\left(\frac{N}{2} - p\right)T_p, \tag{3}$$

The range distance vector from the SAR to the *ijk*-th point scatterer of the target

$$\mathbf{R}_{ijk}(p) = \mathbf{R}_{s0'}(p) + \mathbf{A}\mathbf{R}_{ijk} = \mathbf{R}_{0s}(p) - \mathbf{R}_{00'}(p) + \mathbf{A}\mathbf{R}_{ijk}, \tag{4}$$

where $\mathbf{V}$ and $\mathbf{V}_{0'}$ are the velocity vectors of the carrier and target, respectively, T_p is the azimuth measurement time interval during aperture synthesis, $\mathbf{A}$ is the transformation matrix, $p = \overline{0, N-1}$ is the number of azimuth measurements (segments), T_p is the azimuth measurement time interval during aperture synthesis: p is the current number of azimuth measurements during aperture synthesis, N is the full number of azimuth measurements during aperture synthesis.

3. CW LFM wave form and modeling of deterministic components of SAR signal

CW LFM wave form has the form

$$\dot{S}(t) = \mathbf{exp}\left\{-j\left[\omega t + b(t - mT)^2\right]\right\} \tag{5}$$

where: $\omega = 2\pi\frac{c}{\lambda}$ is the signal angular frequency, $c = 3.10^8$ m/s is the speed of the light. The bandwidth $(2\Delta F)$ of the transmitted pulse provides for the dimension of the range resolution cell, i.e. $\Delta R = c/2\Delta F$, $t = (k-1)\Delta T$, $b = \frac{2\pi\Delta F}{T}$ is the LFM rate, $T = 1.10^{-5}$ s is the half time duration of the triangle modulating pulse voltage, $k = \overline{1, K}$ is the sample number of a CW LFM signal segment; K is the full number of samples of the CW LFM SAR signal segment measured on a range direction, ΔT is the time duration of a LFM sample.

The deterministic component of the CW LFM chirp SAR signal from *ijk*-th scatterer can be expressed by

$$\dot{S}_{ijk}(p,t) = a_{ijk}\,\mathbf{exp}\left\{-j\left[\omega\left(t - t_{ijk}(p)\right) + b\left(t - mT - t_{ijk}(p)\right)^2\right]\right\} \tag{6}$$

The deterministic component of the CW LFM chirp SAR signal from object's scatterer can be expressed by

$$\dot{S}(p,k) = \sum_{ijk} a_{ijk} \exp\left\{ -j\left[\omega\left(t - t_{ijk}(p)\right) + b\left(t - mT - t_{ijk}(p)\right)^2\right]\right\} \quad (7)$$

where a_{ijk} is the reflection coefficient (intensity) of the point scatterer of the target; $t_{ijk}(p) = \dfrac{2R_{ijk}(p)}{c}$ is the time delay of the signal from the ijk th point scatterer of the target.

CW LFM SAR signal formation (7) can be considered as a direct projective operation of an image function onto SAR signal plane For the reference signal in the coherent processing the parameter *m* accepts increasing even values in the following time instant intervals.

$0 \div T$	$T \div 3T$	$3T \div 5T$	$5T \div 7T$	..	$(m-1)T \div (m+1)T$	..	$1998 \div 2001$
$m = 0$	$m = 2$	$m = 4$	$m = 6$	..	$m = m$	..	$m = 2000$

Table: Parameter m time variation

Numerical model of the emitted CW LFM signal (blue) and received signal (red) are illustrated inn Fig. 2. The transmitted signal has a symmetric triangular chirp of period T=20, whose min and max frequencies are 0.5 and 5 respectively.

The interference of the two signals, time frequency dependences of emitted and received signal, and the sum and difference of the emitted and received signals are illustrated in Fig. 3 [13]. Mixer output (a) and spectrum (b) after mixer is presented in Fig. 4. Time dependence of the filtered output after LPF (a) and the spectrum of the filtered output (b) are presented in Fig.

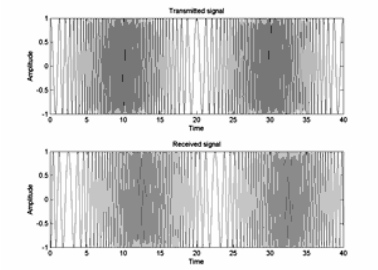

Fig. 2. *Emitted and received CW LFM signal*

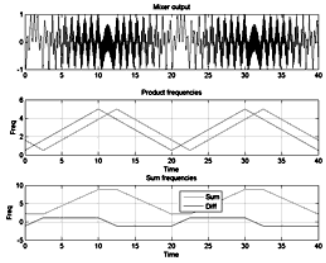

Fig. 3. *Interference, sum and difference of emitted and received CW LFM signal*

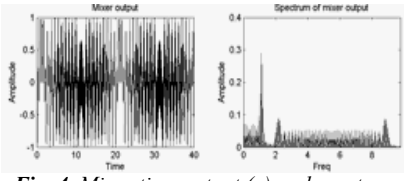

Fig. 4. *Mixer time output (a) and spectrum after mixer (b)*

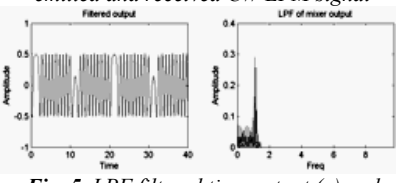

Fig. 5. *LPF filtered time output (a) and spectrum of LPF filtered output*

4. Image reconstruction algorithm

Image reconstruction can be interpreted as inverse projective operation and defined by the expression

(8) $$a_{ijk} = \sum_{p,k} \dot{S}(p,t)\mathbf{exp}\left\{j\left[\omega\left(t - t_{ijk}(p)\right) + b\left(t - mT - t_{ijk}(p)\right)^2\right]\right\}$$

The expression can be reduced to

(9) $$a(\hat{k},\hat{p}) = \sum_{p=1}^{N}\left[\sum_{k=1}^{K}\hat{S}(k,p).\exp\left[j\Phi(k,p)\right].\exp\left(j2\pi\frac{k\hat{k}}{K}\right)\right]\exp\left(j2\pi\frac{p\hat{p}}{N}\right).$$

where $(\hat{k},\hat{p})$ are the coordinates of point scatterers in two dimensional image plane; $\Phi(k,p)$ is the phase correction function, defined iteratively by entropy minimization; $\hat{S}(k,p)$ is the demodulated signal.

Hence, the image extraction algorithm with entropy phase correction can be defined as follows

I. In case $\Phi(k,p) = 0$

1. Range compression by Inverse Fourier transform – IFT $\widetilde{S}(\hat{k},p) = \frac{1}{K}\sum_{k=1}^{K}\widetilde{S}(k,p).\exp\left(j2\pi\frac{k\hat{k}}{K}\right)$

2. Azimuth compression by IFT – $a(\hat{k},\hat{p}) = \frac{1}{N}\sum_{p=1}^{N}\widetilde{S}(\hat{k},p).\exp\left(j2\pi\frac{p\hat{p}}{N}\right).$

$$a(\hat{p},\hat{k}) = \frac{1}{KN}\sum_{p=1}^{N}\left[\sum_{k=1}^{K}\hat{S}(k,p).\exp\left(j2\pi\frac{k\hat{k}}{K}\right)\right]\exp\left(j2\pi\frac{p\hat{p}}{N}\right).$$

II. In case $\Phi(k,p) \neq 0$

1. Phase correction $\widetilde{S}_s(k,p) = \hat{S}(k,p)\exp(-j\Phi_s(p))$.

2. Define polynomial coefficients of the phase correction function $\Phi(p) = a_2.(pT_p)^2 + ... + a_m(pT_p)^m$.

3. Range compression by Inverse Fourier transform (IFT) $\widetilde{S}(\hat{k},p) = \frac{1}{K}\sum_{k=1}^{K}\widetilde{S}(k,p).\exp\left(j2\pi\frac{k\hat{k}}{K}\right).$

4. Azimuth compression by IFT - $a(\hat{k},\hat{p}) = \frac{1}{N}\sum_{p=1}^{N}\widetilde{S}(\hat{k},p).\exp\left(j2\pi\frac{p\hat{p}}{N}\right).$

5. Normalized image function $\hat{a}_s(\hat{p},\hat{k}) = \frac{\left|a_s(\hat{k},\hat{p})\right|^2}{\sum_{p=0}^{N-1}\sum_{k=0}^{K-1}\left|a_s(\hat{k},\hat{p})\right|^2}$.

6. Entropy function $H_s = -\sum_{p=0}^{N-1}\sum_{k=0}^{K-1}\overline{a}_s(\hat{k},\hat{p})\ln[a_s(\hat{k},\hat{p})]$ and polynomial arguments determination

$$a_m = \arg\min_{\mathbf{a}}\left\{H_s[\hat{a}_s(\hat{k},\hat{p})]\right\}$$

5. SAR target image system implementation

Based on electrical scheme of mini SAR system, developed in Massachusetts Institute of Technology, USA presented in Fig. 6, modified SAR system has been created, the output power is 10 mW, carrier frequency is 2.3 GHz, period of triangle modulating voltage is 20 mS. Electrical scheme of the low frequency part of the SAR system is presented in Fig. 7 [13].

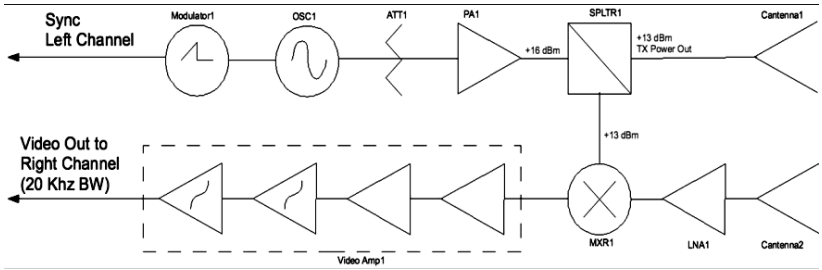

Fig. 6. *Basic elements. Transmitter: modulator, oscillator, attenuator, high frequency (HF) amplifier, HF splitter, transmitter antenna.*
Receiver: receiver antenna, amplifier, mixer, low frequency (LF) amplifier

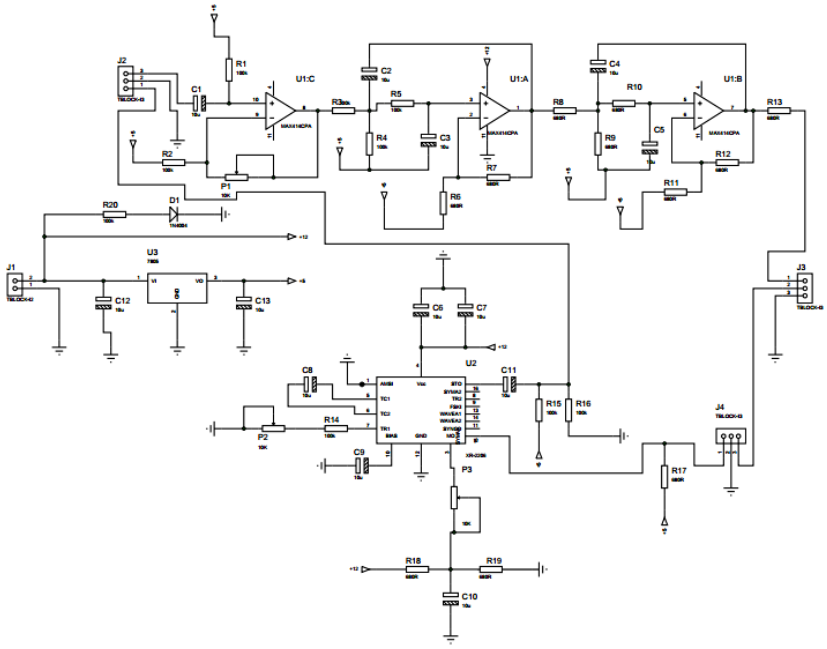

Fig. 7. *Electrical scheme of the low frequency part of the SAR system*

Electrical plate design of LF part is presented in Fig. 8. The implementation of electrical plate of LF part is presented in Fig. 9. The implementation of mini SAR is presented in Fig. 10.

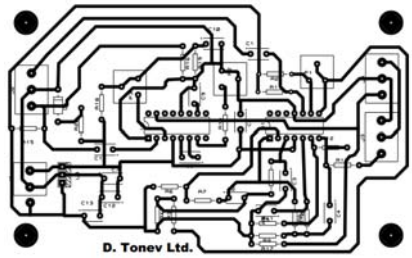

Fig. 8. *Electrical plate design of LF part*

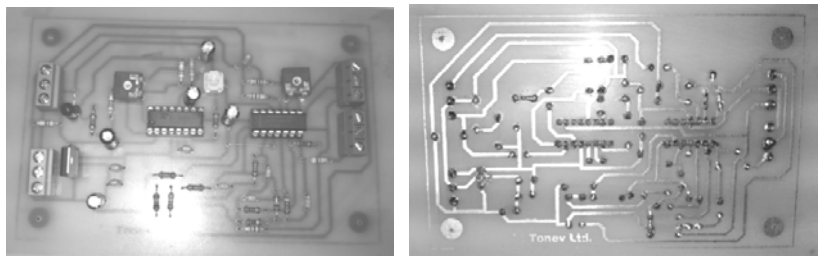

(a) *(b)*

Fig. 9. *Implementation of electrical plate of LF part: view from above (a), view below (b)*

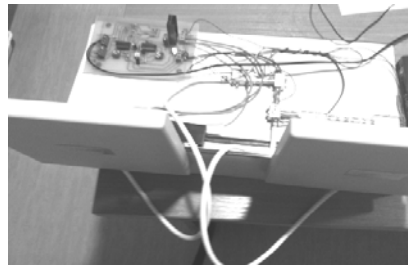

Fig. 10. *Implementation of BFU mini SAR*

In Fig. 11 a range-Doppler image is depicted. A mane is crossing the SAR antenna pattern.

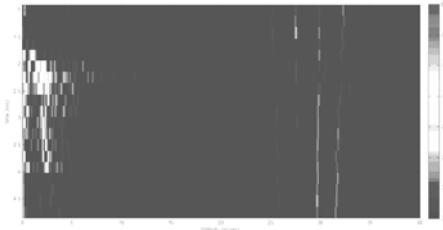

Fig. 11. *Range-Doppler image*

6. Conclusion

SAR problem referred to image reconstruction of a moving target and SAR implementation is considered. Three-dimensional (3-D) SAR geometry is analytically described. The target is presented as an assembly of point scatterers. Mathematical expressions to calculate the range distance from SAR to each point scatterer are derived. SAR signal model based on a linear frequency modulated continuous wave emitted signal, 3-D geometry and reflectivity function of the target is derived. Image reconstruction procedure based on Fourier transform for range compression and azimuth compression is applied. Polynomial autofocusing algorithm for SAR imaging of a moving target is suggested. Mini SAR system is implemented and experimental results are provided.

References

1. C. Elachi, Spaceborne Radar Remote Sensing: Applications and Techniques. New York, NY: IEEE Press, 1987. 2, 29
2. R. O. Harger, Synthetic Aperture Radar Systems: Theory and Design. New York, NY: Academic Press, 1970. 2, 29
3. D. P. Duncan, „Motion compensation of interferometric synthetic aperture radar data," Thesis, Brigham Young University, August 2004. 2
4. M. I. Duersch, „BYU micro-SAR: A very small, low-power LFM-CW synthetic aperture radar," Thesis, Brigham Young University, November 2004. 2, 29
5. A. Currie, „Synthetic aperture radar," Electronics & Communication Engineering Journal, vol. 3, pp. 159–170, August 1991. 2
6. E. Velten and C. Heer, „Future operational spaceborne synthetic aperture radar system considerations," in IEEE International Geoscience and Remote Sensing Symposium, vol. 2, August 1997, pp. 993–995. 2
7. H. B¨ottger, C. Heer, and J. J. W. Wilson, „Design, performance and technology aspects in relation to a next generation high resolution spaceborne sar instrument," in IEEE International Geoscience and Remote Sensing Symposium, vol. 4, May 1996, pp. 2341–2343.
8. V. Adrian and N. Suinot, „CLIMACS: Design of a high radiometric resolution SAR for land and sea ice applications," in IEEE International Geoscience and Remote Sensing Symposium, vol. 3, August 1997, pp. 1150–1152.
9. R. J. Sullivan, Microwave Radar Imaging And Advanced Concepts. Norwood, MA: Artech House, 2000. 2
10. I. G. Cumming and F. H. Wong, Digital Processing of Synthetic Aperture Radar Data: Algorithms and Implementation. Norwood, MA: Artech House, 2005. 2, 20, New York, NY: Wiley-Interscience, 1999. 2
11. E. F. Knott, Radar Cross Section Measurements. New York, NY: Van Nostrand Reinhold, 1993. 3, 76
12. Chan Y. K., V. C. Koo, C. Y. Ang, K. S. Yee, M. Y. Chua. Design and development of a C-band RF transceiver for UAVSAR, In Electro-magnetic Research C, Vol. 24, 2011, pp 1-12.
13. Gregory L. Charvat, MIT IAP 2011 Laptop Based Radar:Block Diagram, Schematics, Bill of Material, and Fabrication Instructions, Presented at the 2011 MIT Independent Activities Period (IAP), MIT Lincoln Laboratory.